

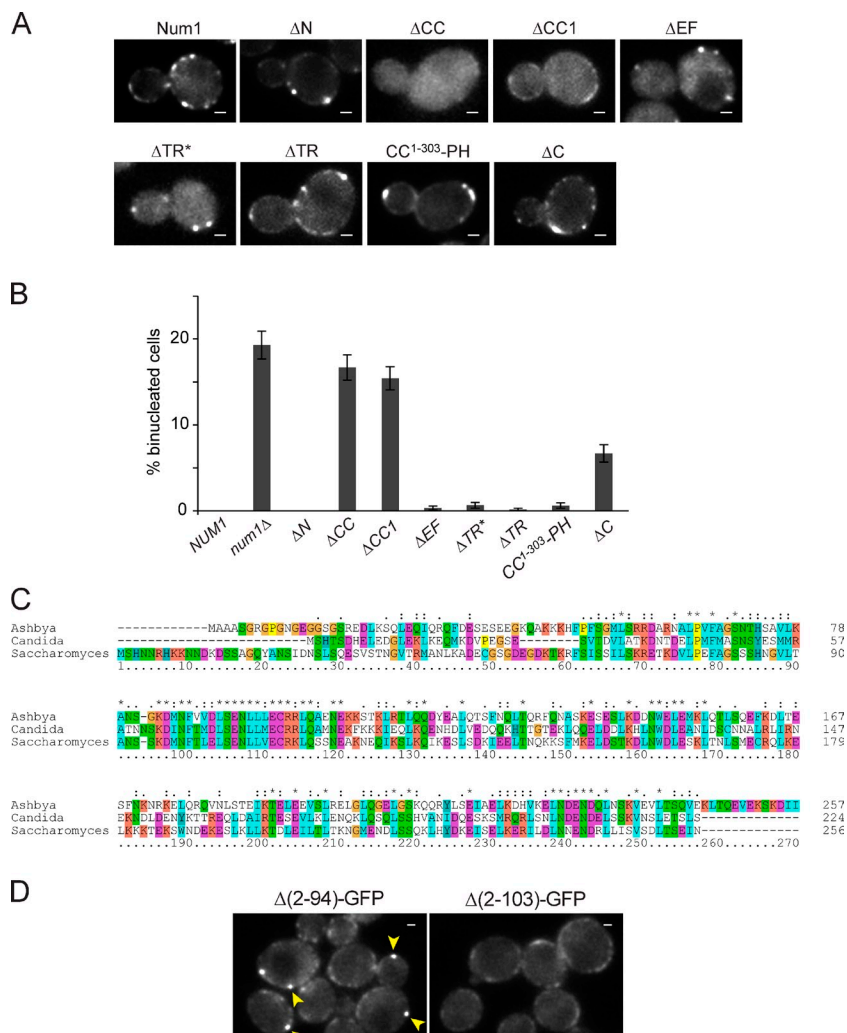
Tang et al., <http://www.jcb.org/cgi/content/full/jcb.201112017/DC1>

Figure S1. Localization and cold nuclear segregation phenotype of various *num1* mutants and an alignment of *Num1* N-terminal sequences from *S. cerevisiae*, *C. glabrata*, and *A. Gossypii*. (A) Widefield single-focal plane images of a live cell expressing GFP-tagged *Num1* mutants schematically shown in Fig. 1. Bars, 1 μ m. (B) The percentage of binucleated cells in cultures grown at 12°C for 16 h. Error bars represent standard error of proportion ($n \geq 495$ cells for each strain). (C) Sequence alignment of the N-terminal regions of *Num1* homologs from *A. Gossypii*, *C. glabrata*, and *S. cerevisiae*. Asterisks, double dots, and single dots indicate identities, conserved substitutions, and semiconserved substitutions, respectively. (D) Widefield single-focal plane images of live cells expressing *Num1* lacking aa 2–94 (left) or aa 2–103 (right) tagged with GFP. Arrowheads indicate bright cortical foci present in Δ (2–94)-GFP cells but absent in Δ (2–103)-GFP cells. Bars, 1 μ m.

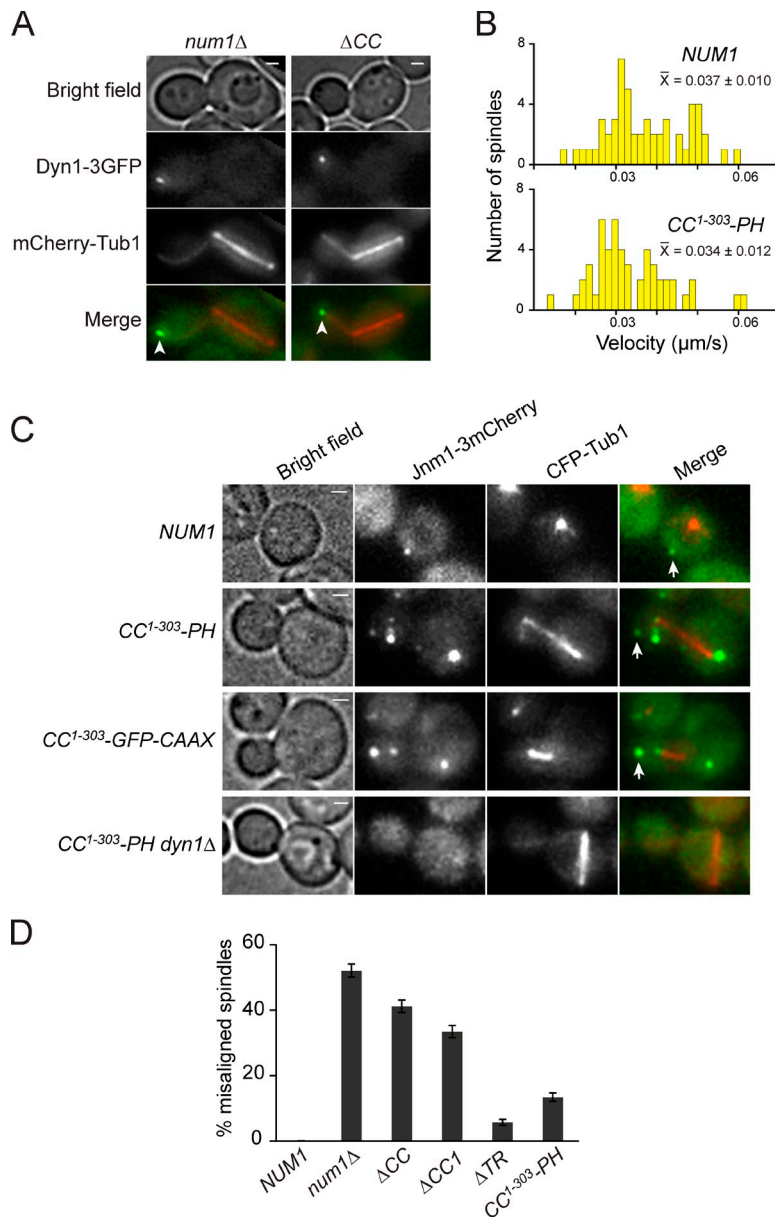


Figure S2. Localization of Dyn1 or Jnm1, distribution of spindle velocity, and cold spindle orientation phenotype of indicated *num1* mutants. (A) ΔCC cells exhibited no cortical Dyn1-3GFP foci. Representative cells of indicated strains expressing Dyn1-3GFP and mCherry-Tub1 are shown. Arrowheads indicate motile Dyn1-3GFP foci at the microtubule plus end. Each image is a maximum intensity projection of a 2- μm z stack of widefield images. Bars, 1 μm . (B) Histograms of the velocity of spindle movement measured in HU-arrested *NUM1* or *CC1-303-PH* cells in the *kar9Δ* background. Velocity is defined as $\Delta D/\Delta T$, in which ΔD is the distance the spindle traveled in a continuous unidirectional movement, and ΔT is the time for the movement ($P = 0.17$ by a *t* test; $n \geq 52$ for each strain from a single experiment). \bar{x} denotes mean \pm SD. (C) *CC1-303-PH* and *CC1-303-GFP-CAAX* cells displayed cortical Jnm1-3mCherry foci. Time-lapse videos were collected at 5-s intervals in cells expressing Jnm1-3mCherry and CFP-Tub1. Cortical foci (indicated by arrows) are defined as those that were not associated with microtubules and remained stationary at the cell cortex for at least three consecutive frames. Each image is a maximum intensity projection of a 2- μm z stack of widefield images. *CC1-303-PH* *dyn1Δ* cells exhibited no plus-end or cortical foci (bottom row). Bars, 1 μm . (D) The percentage of cells with a misaligned spindle after incubation at 12°C for 16 h. Error bars represent standard error of proportion ($n \geq 495$ cells for each strain).

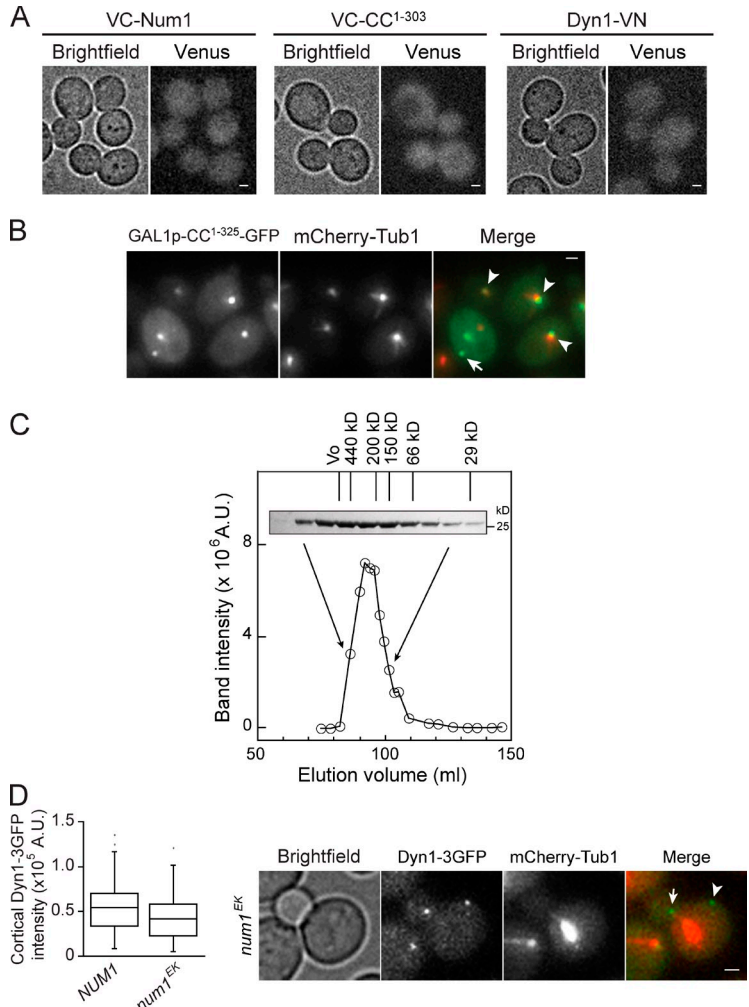


Figure S3. Controls for the BiFC assay, localization of overexpressed CC¹⁻³²⁵-GFP, and functional analysis of *num1^{EK}* mutant. (A) Controls for BiFC assay shown in Fig. 4 B. The N- and C-terminal fragments of Venus, VN and VC, were fused to the C terminus of Dyn1 and the N terminus of Num1 or CC¹⁻³⁰³, respectively. Images of live cells expressing VC-Num1, VC-CC¹⁻³⁰³, or Dyn1-VN were acquired in the YFP channel. Bars, 1 μ m. (B) Live GAL1p-CC¹⁻³²⁵-GFP/NUM1 diploid cells grown in YP media containing galactose. Arrowheads indicate localization of overexpressed CC¹⁻³²⁵-GFP to the SPB. The arrow indicates an aggregated GAL1p-CC¹⁻³²⁵-GFP dot in the cytoplasm (not at the cell cortex), as judged by the corresponding time-lapse data. Bar, 1 μ m. (C) Analytical gel filtration of recombinant CC⁹⁵⁻³⁰³S with E191A + K192A mutation. Purified CC^{95-303(EK)}S was loaded onto a calibrated Sephadryl S-200 column, and fractions were assayed by Coomassie staining. The elution profile of CC^{95-303(EK)}S was similar to that of CC⁹⁵⁻³⁰³S shown in Fig. 6 C. A.U., arbitrary unit. (D) Cortical Dyn1-3GFP foci in *num1^{EK}* cells. (left) Box plot of the intensity of individual cortical Dyn1-3GFP foci in the indicated strains. Lines within each box display the median. Foci in *num1^{EK}* cells were not significantly different from those in wild-type NUM1 cells ($P > 0.2$ by a t test; $n \geq 20$ foci for each strain). (right) A representative *num1^{EK}* cell exhibiting a cortical Dyn1-3GFP focus. The arrow indicates a motile Dyn1-3GFP focus at the microtubule plus end, and the arrowhead indicates a stationary cortical Dyn1-3GFP focus. Each image is a maximum intensity projection of a 2- μ m z stack of widefield images. Bar, 1 μ m.

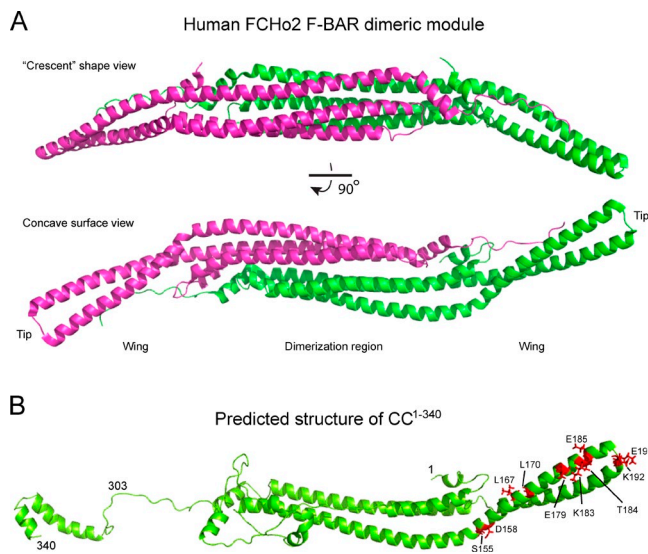
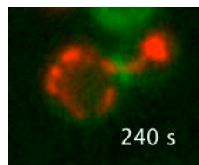
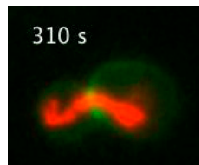


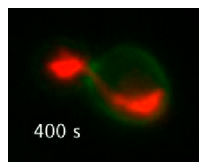
Figure S4. Similarity between CC¹⁻³⁴⁰ and the human FCHO2 F-BAR domain. (A) Crystal structure of the dimeric F-BAR domain of human FCHO2 displayed as a ribbon diagram by PyMOL software using Protein Data Bank accession no. 2v0o [Henne et al., 2007]. The crescent banana shape view (top) and the corresponding 90° view of the concave surface (bottom) are shown. One monomer is magenta, and the other is green. (B) iTASSER (Roy et al., 2010) predicted structure of the N-terminal 1–340 aa of Num1. Residues targeted for point mutation are shown as sticks and are colored in red.



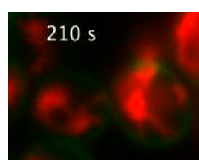
Video 1. Mitochondrial attachment to the cell cortex in wild-type cells. NUM1 cells expressing Cox4-RFP (red) were stained with calcofluor for cell boundary (green). Widefield single focal frames were acquired every 10 s and are displayed at 20 frames/s. The arrowhead indicates the event of mitochondrial division.



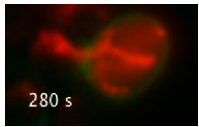
Video 2. Mitochondria are dissociated from the cell cortex in num1Δ mutant. num1Δ cells expressing Cox4-RFP (red) were stained with calcofluor for cell boundary (green). Widefield single focal frames were acquired every 10 s and are displayed at 20 frames/s.



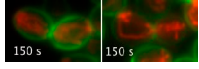
Video 3. Mitochondria are dissociated from the cell cortex in ΔCC1 mutant. ΔCC1 cells expressing Cox4-RFP (red) were stained with calcofluor for cell boundary (green). Widefield single focal frames were acquired every 10 s and are displayed at 20 frames/s.



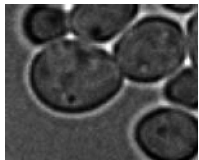
Video 4. Mitochondrial attachment to the cell cortex in CC¹⁻³⁰³.PH cells. CC¹⁻³⁰³.PH cells expressing Cox4-RFP (red) were stained with calcofluor for cell boundary (green). Widefield single focal frames were acquired every 10 s and are displayed at 20 frames/s. The arrowhead indicates the event of mitochondrial division.



Video 5. **Mitochondrial attachment to the cell cortex in CC^{1-303} -GFP-CAAX cells.** CC^{1-303} -GFP-CAAX cells expressing Cox4-RFP (red) were stained with calcofluor for cell boundary (green). Widefield single focal frames were acquired every 10 s and are displayed at 20 frames/s. The arrowhead indicates the event of mitochondrial division.



Video 6. **Mitochondrial attachment to the cell cortex in CC^{1-303} -PH cells does not depend on Dyn1 or Nip100.** CC^{1-303} -PH cells expressing Cox4-RFP (red) were stained with calcofluor for cell boundary (green). Time-lapse images were acquired every 5 s and are displayed at 20 frames/s. Each frame is a maximum intensity projection of a 2- μ m z stack of widefield images. CC^{1-303} -PH $dyn1\Delta$ (left) and CC^{1-303} -PH $nip100\Delta$ (right) are shown.



Video 7. **Cortical attachment of mitochondria in $num1^{\Delta}$ mutant.** $num1^{\Delta}$ cells expressing Cox4-RFP (red) were stained with calcofluor for cell boundary (green). Time-lapse images were acquired every 5 s and are displayed at 20 frames/s. Each frame is a maximum intensity projection of a 2- μ m z stack of widefield images.

Table S1. Yeast strains used in this study

Strain	Genotype	Source
YWL36	MAT α <i>ura3-52 lys2-801 leu2-Δ1 his3-Δ200 trp1-Δ63</i>	Vorvis et al., 2008
YWL37	MAT α <i>ura3-52 lys2-801 leu2-Δ1 his3-Δ200 trp1-Δ63</i>	Vorvis et al., 2008
YWL484	MAT α <i>kar9Δ::TRP1 ura3-52 lys2-801 leu2-Δ1 his3-Δ200 trp1-Δ63</i>	This study
YWL555	MAT α <i>num1Δ::HIS3 ura3-52 lys2-801 leu2-Δ1 his3-Δ200 trp1-Δ63</i>	This study
YWL630	MAT α <i>NUM1-GFP::spHIS5 ura3-52 lys2-801 leu2-Δ1 his3-Δ200 trp1-Δ63</i>	This study
YWL631	MAT α <i>num1ΔC::spHIS5 ura3-52 lys2-801 leu2-Δ1 his3-Δ200 trp1-Δ63</i>	This study
YWL670	MAT α <i>num1Δ::GFP-CAAX::spHIS5 ura3-52 lys2-801 leu2-Δ1 his3-Δ200 trp1-Δ63</i>	This study
YWL704	MAT α <i>NUM1-GFP::spHIS5 ura3-52::mCherry-TUB1::URA3 lys2-801 leu2-Δ1 his3-Δ200 trp1-Δ63</i>	This study
YWL714	MAT α <i>dyn1_{TAI}-3GFP::TRP1 ura3-52 lys2-801 leu2-Δ1 his3-Δ200 trp1-Δ63</i>	Markus et al., 2009
YWL754	MAT α <i>dyn1_{TAI}-3GFP::TRP1 nip100Δ::HIS3 ura3-52 lys2-801 leu2-Δ1 his3-Δ200 trp1-Δ63</i>	This study
YWL854	MAT α/α <i>ura3-52::CFP-TUB1::URA3/ura3-52 lys2-801/lys2-801 leu2-Δ1/leu2-Δ1 his3-Δ200/trp1-Δ63/trp1-Δ63</i>	This study
YWL1090	MAT α <i>num1ΔEF-GFP-6xHIS::TRP1 ura3-52 lys2-801 leu2-Δ1 his3-Δ200 trp1-Δ63</i>	This study
YWL1095	MAT α <i>PH-GFP-6xHIS::TRP1 ura3-52 lys2-801 leu2-Δ1 his3-Δ200 trp1-Δ63</i>	Tang et al., 2009
YWL1098	MAT α <i>num1ΔTR*-GFP-6xHIS::TRP1 ura3-52 lys2-801 leu2-Δ1 his3-Δ200 trp1-Δ63</i>	This study
YWL1105	MAT α <i>num1ΔPH-GFP-6xHIS::TRP1 ura3-52 lys2-801 leu2-Δ1 his3-Δ200 trp1-Δ63</i>	This study
YWL1221	MAT α <i>CC¹⁻³⁰³-PH-GFP::spHIS5 ura3-5 lys2-801 leu2-Δ1 his3-Δ200 trp1-Δ63</i>	This study
YWL2009	MAT α <i>num1ΔCC-GFP::spHIS5 ura3-52 lys2-801 leu2-Δ1 his3-Δ200 trp1-Δ63</i>	This study
YWL2076	MAT α <i>Jnm1-3mCherry::HIS3 GFP-TUB1::LEU2 ura3-5 lys2-801 leu2-Δ1 his3-Δ200 trp1-Δ63</i>	This study
YWL2183	MAT α <i>num1Δ(2-103)-GFP::spHIS5 ura3-52 lys2-801 leu2-Δ1 his3-Δ200 trp1-Δ63</i>	This study
YWL2228	MAT α <i>Dyn1-3GFP::TRP1 ura3-52::MET3p-mCherry-TUB1::URA3 lys2-801 leu2-Δ1 his3-Δ200 trp1-Δ63</i>	This study
YWL2250	MAT α <i>num1ΔCC1-GFP::spHIS5 ura3-52 lys2-801 leu2-Δ1 his3-Δ200 trp1-Δ63</i>	This study
YWL2259	MAT α <i>num1ΔTR-GFP::spHIS5 ura3-52 lys2-801 leu2-Δ1 his3-Δ200 trp1-Δ63</i>	This study
YWL2287	MAT α <i>num1Δ::HIS3 Dyn1-3GFP::TRP1 ura3-52::MET3p-mCherry-TUB1::URA3 lys2-801 leu2-Δ1 his3-Δ200 trp1-Δ63</i>	This study
YWL2317	MAT α <i>num1ΔCC::LEU2 Dyn1-3GFP::TRP1 ura3-52::MET3p-mCherry-TUB1::URA3 lys2-801 leu2-Δ1 his3-Δ200 trp1-Δ63</i>	This study
YWL2355	MAT α <i>num1ΔC::LEU2 Dyn1-3GFP::TRP1 ura3-52::MET3p-mCherry-TUB1::URA3 lys2-801 leu2-Δ1 his3-Δ200 trp1-Δ63</i>	This study
YWL2366	MAT α <i>CC¹⁻³⁰³-PH::LEU2 Dyn1-3GFP::TRP1 ura3-52::MET3p-mCherry-TUB1::URA3 lys2-801 leu2-Δ1 his3-Δ200 trp1-Δ63</i>	This study
YWL2406	MAT α <i>num1ΔTR::LEU2 Dyn1-3GFP::TRP1 ura3-52::MET3p-mCherry-TUB1::URA3 lys2-801 leu2-Δ1 his3-Δ200 trp1-Δ63</i>	This study
YWL2407	MAT α <i>num1ΔCC1::LEU2 Dyn1-3GFP::TRP1 ura3-52::MET3p-mCherry-TUB1::URA3 lys2-801 leu2-Δ1 his3-Δ200 trp1-Δ63</i>	This study
YWL2589	MAT α <i>DYN1-VN::HIS3 ura3-52::CFP-TUB1::URA3 lys2-801 leu2-Δ1 his3-Δ200 trp1-Δ63</i>	This study
YWL2729	MAT α <i>CC¹⁻³⁰³-GFP::spHIS5 ura3-52 lys2-801 leu2-Δ1 his3-Δ200 trp1-Δ63</i>	This study
YWL2827	MAT α <i>PAC11-13Myc::TRP1 ura3-52 lys2-801 leu2-Δ1 his3-Δ200 trp1-Δ63</i>	This study
YWL2876	MAT α <i>PAC11-13Myc::TRP1 nip100Δ::HIS3 ura3-52 lys2-801 leu2-Δ1 his3-Δ200 trp1-Δ63</i>	This study
YWL2997	MAT α <i>CC¹⁻³⁰³-GFP-CAAX::spHIS5 ura3-52 lys2-801 leu2-Δ1 his3-Δ200 trp1-Δ63</i>	This study
YWL3017	MAT α/α <i>KAN^R::GAL1p-CC¹⁻³²⁵-13Myc-HIS3/NUM1 GFP-TUB1::LEU2 ura3-52/ura3-52 lys2-801/lys2-801 leu2-Δ1/leu2-Δ1 his3-Δ200/his3-Δ200 trp1-Δ63/trp1-Δ63</i>	This study
YWL3018	MAT α/α <i>KAN^R::GAL1p-CC¹⁻³²⁵-13Myc-HIS3/NUM1 GFP-TUB1::LEU2 ura3-52/ura3-52 lys2-801/lys2-801 leu2-Δ1/leu2-Δ1 his3-Δ200/his3-Δ200 trp1-Δ63/trp1-Δ63</i>	This study
YWL3019	MAT α/α <i>num1Δ::HIS3/NUM1 GFP-TUB1::LEU2 ura3-52/ura3-52 lys2-801/lys2-801 leu2-Δ1/leu2-Δ1 his3-Δ200/his3-Δ200 trp1-Δ63/trp1-Δ63</i>	This study
YWL3021	MAT α/α <i>num1Δ::HIS3/num1Δ::HIS3 DYN1-3GFP::TRP1/DYN1 ura3-52::CFP-TUB1::URA3/ura3-52 lys2-801/lys2-801 leu2-Δ1/leu2-Δ1 his3-Δ200/his3-Δ200 trp1-Δ63/trp1-Δ63</i>	This study
YWL3048	MAT α/α <i>DYN1-3mCherry::HIS3/DYN1 GFP-TUB1::LEU2 ura3-52/ura3-52 lys2-801/lys2-801 leu2-Δ1/leu2-Δ1 his3-Δ200/his3-Δ200 trp1-Δ63/trp1-Δ63</i>	This study
YWL3050	MAT α/α <i>DYN1-3GFP::TRP1/DYN1 num1Δ::HIS3/num1Δ::HIS3 COX4-mCherry::URA3/COX4 GFP-TUB1::LEU2 ura3-52/ura3-52 lys2-801/lys2-801 leu2-Δ1/leu2-Δ1 his3-Δ200/his3-Δ200 trp1-Δ63/trp1-Δ63</i>	This study
YWL3052	MAT α/α <i>CC¹⁻³²⁵-13Myc::HIS3/NUM1 GFP-TUB1::Leu ura3-52/ura3-52 lys2-801/lys2-801 leu2-Δ1/leu2-Δ1 his3-Δ200/his3-Δ200 trp1-Δ63/trp1-Δ63</i>	This study
YWL3054	MAT α <i>VC-NUM1::TRP1 ura3-52 lys2-801 leu2-Δ1 his3-Δ200 trp1-Δ63</i>	This study
YWL3056	MAT α <i>VC-CC¹⁻³⁰³::TRP1 ura3-52 lys2-801 leu2-Δ1 his3-Δ200 trp1-Δ63</i>	This study
YWL3098	MAT α/α <i>KAN^R::GAL1p-CC¹⁻³²⁵-13Myc-HIS3/KAN^R::GAL1p-CC¹⁻³²⁵-3HA-TRP1 ura3-52/ura3-52 lys2-801/lys2-801 leu2-Δ1/leu2-Δ1 his3-Δ200/his3-Δ200 trp1-Δ63/trp1-Δ63</i>	This study

Table S1. Yeast strains used in this study (Continued)

Strain	Genotype	Source
YWL3100	MAT α KAN R ::GAL1p-CC ¹⁻³²⁵ 3HA-TRP1/NUM1 TUB1-GFP::LEU2 ura3-52/ura3-52 lys2-801/lys2-801 leu2-Δ1/leu2-Δ1 his3-Δ200/his3-Δ200 trp1-Δ63/trp1-Δ63	This study
YWL3107	MAT α DYN1-VN::HIS3 VC-NUM1::TRP1 ura3-52::CFP-TUB1::URA3 lys2-801 leu2-Δ1 his3-Δ200 trp1-Δ63	This study
YWL3111	MAT α DYN1-VN::HIS3 VC-CC ¹⁻³⁰³ ::TRP1 ura3-52::CFP-TUB1::URA3 lys2-801 leu2-Δ1 his3-Δ200 trp1-Δ63	This study
YWL3135	MAT α num1ΔCC1-GFP::spHIS5 ura3-52 lys2-801 leu2-Δ1 his3-Δ200 trp1-Δ63 [pHS78 (COX4-RFP)]	This study
YWL3137	MAT α CC ¹⁻³⁰³ -GFP-CAAX::spHIS5 ura3-52 lys2-801 leu2-Δ1 his3-Δ200 trp1-Δ63 [pHS78 (COX4-RFP)]	This study
YWL3141	MAT α num1Δ::HIS3 ura3-52 lys2-801 leu2-Δ1 his3-Δ200 trp1-Δ63 [pHS78 (COX4-RFP)]	This study
YWL3145	MAT α CC ¹⁻³⁰³ -PH-GFP::spHIS5 ura3-5 lys2-801 leu2-Δ1 his3-Δ200 trp1-Δ63 [pHS78 (COX4-RFP)]	This study
YWL3148	MAT α NUM1-GFP::spHIS5 ura3-52 lys2-801 leu2-Δ1 his3-Δ200 trp1-Δ63 [pHS78 (COX4-RFP)]	This study
YWL3188	MAT α Kan R ::GAL1p-CC ¹⁻³²⁵ -yEGFP::spHIS5/NUM1 ura3-52::MET3p-mCherry-TUB1::URA3/ura3-52 lys2-801/lys2-801 leu2-Δ1/leu2-Δ1 his3-Δ200/his3-Δ200 trp1-Δ63/trp1-Δ63	This study
YWL3237	MAT α num1ΔN-GFP::spHIS5 ura3-52 lys2-801 leu2-Δ1 his3-Δ200 trp1-Δ63	This study
YWL3277	MAT α kar9Δ::TRP1 ura3-52::MET3p-mCherry-TUB1::URA3 lys2-801 leu2-Δ1 his3-Δ200 trp1-Δ63	This study
YWL3701	MAT α CC ¹⁻³⁰³ -GFP-CAAX::spHIS5 dyn1Δ::TRP1 ura3-52 lys2-801 leu2-Δ1 his3-Δ200 trp1-Δ63 [pHS78 (COX4-RFP)]	This study
YWL3702	MAT α CC ¹⁻³⁰³ -PH-GFP::spHIS5 dyn1Δ::TRP1 ura3-5 lys2-801 leu2-Δ1 his3-Δ200 trp1-Δ63 [pHS78 (COX4-RFP)]	This study
YWL3704	MAT α NUM1-GFP::spHIS5 dyn1Δ::TRP1 ura3-52 lys2-801 leu2-Δ1 his3-Δ200 trp1-Δ63 [pHS78 (COX4-RFP)]	This study
YWL3706	MAT α CC ¹⁻³⁰³ -PH-GFP::spHIS5 nip100Δ::URA3 ura3-52 lys2-801 leu2-Δ1 his3-Δ200 trp1-Δ63 [pHS78 (COX4-RFP)]	This study
YWL3708	MAT α NUM1-GFP::spHIS5 nip100Δ::URA3 ura3-52 lys2-801 leu2-Δ1 his3-Δ200 trp1-Δ63 [pHS78 (COX4-RFP)]	This study
YWL3711	MAT α CC ¹⁻³⁰³ -PH-GFP::spHIS5 GFP-TUB1::LEU2 kar9Δ::TRP1 ura3-5 lys2-801 leu2-Δ1 his3-Δ200 trp1-Δ63	This study
YWL3713	MAT α GFP-TUB1::LEU2 kar9Δ::TRP1 ura3-5 lys2-801 leu2-Δ1 his3-Δ200 trp1-Δ63	This study
YWL3716	MAT α CC ¹⁻³⁰³ -GFP-CAAX::spHIS5 nip100Δ::URA3 ura3-52 lys2-801 leu2-Δ1 his3-Δ200 trp1-Δ63 [pHS78 (COX4-RFP)]	This study
YWL3738	MAT α num1 ^{L167E + L170E} -GFP::spHIS5 ura3-52 lys2-801 leu2-Δ1 his3-Δ200 trp1-Δ63	This study
YWL3740	MAT α num1 ^{E191A + K192A} -GFP::spHIS5 ura3-52 lys2-801 leu2-Δ1 his3-Δ200 trp1-Δ63	This study
YWL3748	MAT α CC ¹⁻³⁰³ -GFP-CAAX::spHIS5 Jnm1-3mCherry::HIS3 ura3-52::CFP-TUB1::URA3 ura3-5 lys2-801 leu2-Δ1 his3-Δ200 trp1-Δ63	This study
YWL3749	MAT α CC ¹⁻³⁰³ -PH-GFP::spHIS5 Jnm1-3mCherry::HIS3 ura3-52::CFP-TUB1::URA3 ura3-5 lys2-801 leu2-Δ1 his3-Δ200 trp1-Δ63	This study
YWL3772	MAT α CC ¹⁻³⁰³ -PH-GFP::spHIS5 dyn1Δ::TRP1 Jnm1-3mCherry::HIS3 ura3-52::CFP-TUB1::URA3 ura3-5 lys2-801 leu2-Δ1 his3-Δ200 trp1-Δ63	This study
YWL3775	MAT α num1 ^{L167E + L170E} -GFP::spHIS5 Jnm1-3mCherry::HIS3 ura3-52::CFP-TUB1::URA3 lys2-801 leu2-Δ1 his3-Δ200 trp1-Δ63	This study
YWL3787	MAT α num1 ^{E191A + K192A} -GFP::spHIS5 kar9Δ::TRP1 ura3-52::MET3p-mCherry-TUB1::URA3 lys2-801 leu2-Δ1 his3-Δ200 trp1-Δ63	This study
YWL3795	MAT α num1 ^{L167E + L170E} -GFP::spHIS5 Dyn1-3GFP::TRP1 ura3-52::MET3p-mCherry-TUB1::URA3 lys2-801 leu2-Δ1 his3-Δ200 trp1-Δ63	This study
YWL3797	MAT α num1 ^{E191A + K192A} -GFP::LEU2 Dyn1-3GFP::TRP1 ura3-52::MET3p-mCherry-TUB1::URA3 lys2-801 leu2-Δ1 his3-Δ200 trp1-Δ63	This study

Table S2. Primers for constructing *num1* mutants

Mutant	Primer name	Primer sequence
$\Delta CC1$	F1	5'-TCCCACAATGGAGTACTCACGGCGAATTCAAAAGGATATGAACTTACTTGG- AACTACCTGATGCGGTATTTCTCC-3'
	R1	5'-TAATGTTAAAATTCCAAATCTGTTTCAGAAGTTCAGGTTCTTTCATCATTCCAT- AACTATGCGGCATCAGAGC-3'
	F2	5'-TCCCACAATGGAGTACTCACGGCGAATTCAAAAGGATATGAACTTACTTGGAAC- TATGGAATGATGAAAAAGAAAGCCTG-3'
	R2	5'-GTCTTCTTCACTAGTGGTCCCC-3'
ΔCC	F1	5'-CAACAGGCATAAAAAGAACGATAAAAGACAGCTCAGCAGGGCAGTATGCAAATA- GCATTCTGATGCGGTATTTCTCC-3'
	R1	5'-GGTCCCCCTCAGAACGATCAGATGTTACTGTAGTATCGGAAGTATGCTTTGATAT- AACTATGCGGCATCAGAGC-3'
	F2	5'-CAACAGGCATAAAAAGAACGATAAAAGACAGCTCAGCAGGGCAGTATGCAAATA- GCATTATCAAAACAGCATACTTCCGATAC-3'
	R2	5'-CAGCCGTTCTCTCCAGCC-3'
ΔTR	F1	5'-CTAAGAGAAAAGCTCTGCATCAGATTATTACTCAAAAAAGAAGACTACGTGA- GCCCTGATGCGGTATTTCTCC-3'
	R1	5'-CTTAAACAAATATCCCCAATGACGGTTGGGTAACGGGGTATTATGCTGGTCGTT- GCACCACGCTTCAATTCAATT-3'
	F2	5'-GATTGCCTGATAATACCTAC-3'
	R2	5'-CTTAAACAAATATCCCCAATGACGGTTGGGTAACGGGGTATTATGCTGGTCGTT- GCTCACGTAGTCTCTTTGAG-3'
$CC^{1-303}.PH$	F1	5'-AGAAAAGTACAAAAGAAGTATTATCAAAAACAGCATACTCCGATACTACAGTAACATC- TCATCTGTGCGGTATTCACACCGC-3'
	R1	5'-CTTAAACAAATATCCCCAATGACGGTTGGGTAACGGGGTATTATGCTGGTCGTTG- CACCACGCTTCAATTCAATT-3'
	F2	5'-GCGAGAATTGTTGGTGAGTG-3'
	R2	5'-CTTAAACAAATATCCCCAATGACGGTTGGGTAACGGGGTATTATGCTGGTCGTTA- GATTTACTGTAGTATCGGAAGTATGC-3'

References

- Henne, W.M., H.M. Kent, M.G. Ford, B.G. Hegde, O. Daumke, P.J. Butler, R. Mittal, R. Langen, P.R. Evans, and H.T. McMahon. 2007. Structure and analysis of FChO2 F-BAR domain: A dimerizing and membrane recruitment module that effects membrane curvature. *Structure*. 15:839–852. <http://dx.doi.org/10.1016/j.str.2007.05.002>
- Markus, S.M., J.J. Punch, and W.L. Lee. 2009. Motor- and tail-dependent targeting of dynein to microtubule plus ends and the cell cortex. *Curr. Biol.* 19:196–205. <http://dx.doi.org/10.1016/j.cub.2008.12.047>
- Roy, A., A. Kucukural, and Y. Zhang. 2010. I-TASSER: A unified platform for automated protein structure and function prediction. *Nat. Protoc.* 5:725–738. <http://dx.doi.org/10.1038/nprot.2010.5>
- Tang, X., J.J. Punch, and W.L. Lee. 2009. A CAAX motif can compensate for the PH domain of Num1 for cortical dynein attachment. *Cell Cycle*. 8:3182–3190. <http://dx.doi.org/10.4161/cc.8.19.9731>
- Vorvis, C., S.M. Markus, and W.L. Lee. 2008. Photoactivatable GFP tagging cassettes for protein-tracking studies in the budding yeast *Saccharomyces cerevisiae*. *Yeast*. 25:651–659. <http://dx.doi.org/10.1002/yea.1611>